GEODESY

UDC 528.482:004.052

Kornyliy TRETYAK[1a], Bogdan PALIANYTSIA[1b]

[1*] Department of Higher Geodesy and Astronomy, Lviv Polytechnic National University, 12, S. Bandery Str., Lviv, 79013, Ukraine, e-mail: bohdan.b.palianytsia@lpnu.ua, [1a] https://orcid.org/0000-0001-5231-3517, [1b] https://orcid.org/0000-0003-4203-1043

https://doi.org/10.23939/jgd2021.01.005

RESEARCH OF SEASONAL DEFORMATIONS OF THE DNIPRO HPP DAM ACCORDING TO GNSS MEASUREMENTS

The goal. Identify the relationship between seasonal temperature changes and vertical and horizontal displacements of GNSS control points based on data obtained by the automated monitoring system of the Dnipro HPP dam in the period from 2016 to 2020. Input data. The research used data of uninterrupted GNSS measurements obtained at 16 points of the Dnipro HPP dam from mid-2016 to mid-2020. Method. A specially developed software product analyzes the GNSS time series of measurements pre-processed by the GeoMoS system to determine the parameters of seasonal displacements and their relationship with seasonal changes in air temperature. The GNSS time series analysis. Based on the conducted research, the influence of environmental temperature has a decisive effect on the cyclicity of dam deformations. This applies to both horizontal and vertical displacements but in the absence of significant changes in the water level in the upper reservoir. Values of extreme displacements increase closer to the middle of the dam and decrease at the edges. This tendency is observed every year in the study period. According to the three-year GNSS dam monitoring, the amplitude of semi-annual horizontal oscillations of the control points relative to the dam axis is in the range of 15-18 mm. Almost all vectors of horizontal displacements are perpendicular to the axis of the arcuate dam. In the first half of the year, the vectors of horizontal displacements aim to widen the dam, and in the second half of the year – at compressing the dam. The analysis of the data represents that almost every year, extreme deviations, both horizontal and vertical, occur in February and August. Temperature extremes occur faster than excessive GNSS displacements. For the dam of the Dnipro HPP, the extreme horizontal displacements lag on average by 37 days, and the vertical ones – by 32 days from the extreme temperatures. The deformations of the dam are related to the concrete structure temperature, which changes with a certain delay relative to the air temperature. The magnitudes of extreme displacements and the epoch of their manifestation depend on the dam's design and its technical parameters. For each dam, these extreme displacements and the periods of their representation will be different. Accordingly, monitoring these displacements and their changes over time is one of the criteria for assessing the general condition of the dam. Scientific novelty and practical significance. The regularities of the connection between the change of temperature and the displacements of the GNSS points, revealed during the research, can be used for the further study of data processing and analysis of the hydraulic structures monitoring.

Key words: GNSS measurements, geodetic monitoring of hydraulic structures, geodetic monitoring of the Dnipro HPP.

Introduction

Dams are essential hydraulic structures necessary to provide humanity with environmentally-friendly electricity, create water reserves, and store waste from environmental pollution. The built-up dams also pose a particular danger to the environment. [Chrzanowski, et al., 2011, Khosravi, et al., 2013; Sarkar, et al., 2013; Zeidan, 2015; Zhang, L. et al., 2015]. Changes in the water level in artificial reservoirs during floods and technical operations cause hydrodynamic loads on the surrounding areas and the earth's crust, which can cause seismicity that can destroy the dam itself. Dam aging during long periods of operation causes deformations, stresses, and cracks in concrete structures, which is dangerous for the dam's stability. According to the International Commission on Large Dams (ISOLD), up to 80 % of all catastrophic destruction of river hydraulic structures occurred under the influence of these factors [National Report on the State of Man-Made and Natural Safety in Ukraine in 2013].

Among all hydraulic structures, dams of large reservoirs have the most severe hydrodynamic man-caused risk for the population and territories in terms of probable dangerous consequences.

In Ukraine, hydropower is highly developed. There are 6 hydro units on the Dnipro River, including the Dnipro Hydro Unit which is the most powerful one (1569 MW). It is located on the Dnipro River in Zaporizhia above Fr. Khortytsia in a relatively narrow valley (Fig. 1).

The bottom and banks of the river valley in this area form an array of medium- and coarse-grained Archean granites. The basis of the Dnipro HPP structures (Fig. 2) is crystalline rocks of the Zaporizhia block, represented mainly by weakly weathered granites with increased fracture.

The idea of building a dam on the Dnipro River originated in the eighteenth century. It can be considered

as a symbol of an entire era, which still arouses admiration for its beauty and grandeur.

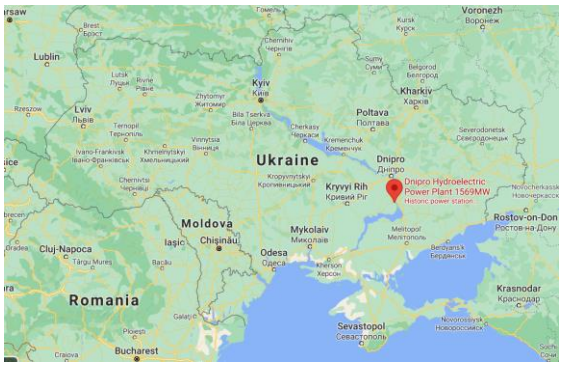

Fig. 1. Fragment of a map with the location of the Dnipro HPP.

Fig. 2. Drainage dam of the Dnipro HPP.

The average annual electricity produced by the Dnipro HPP is about 4008 million kWh. Construction of the power plant began in 1927, and in 1932 was opened. The size of the dam is impressive: length – 760 m, height – 60 m. During the Second World War in 1941 and 1943, the dam was blown up twice [Moroko. 2010]. Even before the end of the Second World War in 1944, the reconstruction of the hydroelectric power plant began, and in March 1947, the first unit of the Dnipro HPP was put into operation. As of today, 17 turbines are operating.

Constant monitoring of the technical condition of the dam is required, taking into account the extent of the destruction. One of the methods of assessing the stability of the dam is geodetic monitoring. The structural complexity of these engineering constructions requires a careful approach to creating a monitoring system [Chen, et al., 1990]. The purpose of monitoring is to prevent severe accidents and damage and collect data to verify design parameters, study the causes of deformation processes, and gain experience to create new and more advanced projects [Chrzanowski et al. 2011]. Monitoring technologies have been improving for a long time. The accuracy of collecting and measuring information is constantly increasing, and the degree of automation of data processing is progressing. The use of the latest ground and space technologies makes it possible to obtain a long-time series of high-precision observations. This significantly improves the quality of monitoring of hydraulic structures [Milillo, et al. 2016].

Methods based on Global Navigation Satellite Systems (GNSS) were at first widely used just for measuring displacements at dam points. Then GNSS networks which were used for periodic measurements at controlled reference points were created. In recent years, automated control systems (ACS) and integrated systems have been developed. Automated systems collect signals from the GNSS receivers capable of operating in a continuous mode. Integrated systems with other means of monitoring are included in the system of early warning of threats to the safe operation of hydraulic structures [Drummond, 2010; Scaioni, et al., 2018]. The obtained integrated data are actively used for analysis and representation of deformation processes at hydropower facilities.

Monitoring data are used for research applying statistical, deterministic methods and structural modelling of correlation with external loads, for example, changes in water levels in the reservoir, seasonal changes in environmental conditions, etc. [Chrzanowski, et al., 2011; Corsetti, et al., 2018]. Many authors [Yunlong. et al., 2018; Oro, SR., et al., 2016; Mata. et al., 2013, and others] argue that one of the leading causes of seasonal deformation of dams is the dynamics in annual air temperature change, provided that the water level in the reservoir does not change significantly.

A sinusoidal function represents the annual variation of the Alto Lindoso concrete dam in Portugal (length 297 m, height 110 m) and the effect of changes in concrete temperature [Mata, et al., 2013], the argument of which is the ordinal number of the day from the beginning of the year to the observation date. An annual heatwave is constructed without taking into account daily temperature variations; as such data are difficult to relate to the nature of the signal and the response of the dam.

The results of the monitoring of the arch dam of Lijiaxia HPP (length of the central section 204 m, height 147 m), located on the Chinese Yellow River [Zhang,. et al., 2018], did not reveal correlations between dam deformations and water level fluctuations, but only from seasonal temperature changes. It was found that when the temperature reached its highest value in July 2015, the arched dam expanded, moving upstream, and its creep was maximum. In January – on the contrary, the dam was compressed, moving downstream. The displacement in the middle was about 10 mm, and at the edges – about 5,3 mm.

At the dam of the Dnipro HPP, monitoring of spatial movements by GNSS methods began in 1997. The results of observations showed that the top of the dam has regular cyclic movements. Further observations were needed to establish the range of these movements and to accumulate relevant data. Thenceforth, various physical indicators are constantly monitored, and different geodetic measurements are carried out to control the condition of

the hydraulic structure. [Tretyak, et al., 2015]. Since 2015, the Dnipro HPP has been operating a stationary system for monitoring the spatial displacement of buildings. The software of this system is the software products of Leica GeoMoS and Spider. Since the launch of the automated system, the efficiency of data acquisition has significantly increased, monitoring has begun to be carried out automatically.

The stationary system of monitoring of spatial displacements of constructions is a modern software and hardware complex. It collects and transmits the results of measurements to the server from multisystem GNSS receivers, robotic electronic total stations, precision inclinometers, and other equipment. To determine the reliable parameters of displacements and deformations of the GNSS dam, the measurements are processed using the Spider software product and transmitted to the GeoMoS software product for joint processing with other geodetic and geotechnical sensors. The scheme of the GeoMoS system is shown in Fig. 3.

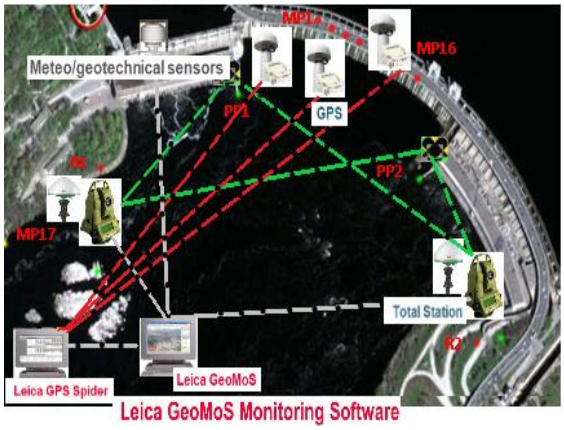

Fig. 3. Scheme of the stationary system for monitoring the spatial displacements of the Dnipro HPP buildings.

The monitoring system of the Dnipro HPP contains 63 points located on the dam and important buildings. The coordinates of MP01-MP17, R1, and R2 are determined by satellite and linear-angular measurements; they are equipped with GNSS receivers and 360º reflectors. Points R1 and R2 are additionally equipped with electronic robotic total stations and points PP1 and PP2 – reflectors for linear-angular measurements (measurement data from total stations are not considered in this work).

The goal

The aim is to identify the relationship between seasonal temperature changes and vertical and horizontal displacements of GNSS points based on data obtained by the automated monitoring system of the Dnipro HPP dam in the period from 2016 to 2020.

Input data

The GNSS data of measurements carried out at the points of the Dnipro HPP dam were used for the research. The location of the items is represented in Fig. 4.

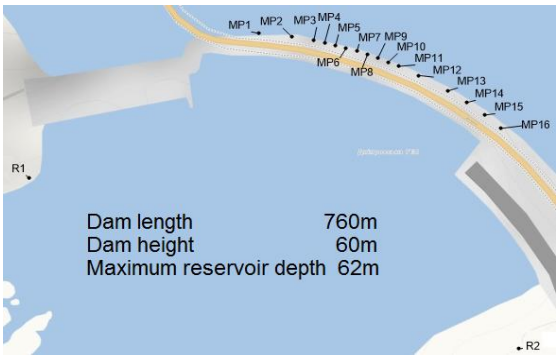

Fig. 4. GNSS network of points on the dam of the Dnipro HPP.

a – fundamental geodetic point R1

b – *monitoring* point MP-4

Fig. 5. General view of items.

Directly on the dam, there are 16 monitoring points (MP1-MP16), where round-the-clock GNSS observations are carried out (from point MP-9 the information was not received), and two fundamental geodetic points R1 s R2, equipped with GNSS receivers Leica GMX902 GG with AR10 antenna, robotic total station TM30, Nivel 201 precision inclinometer, and DTM meteorological sensor. The tubes to which the antennas are mounted shall be protected against the effects of ambient temperature, ultraviolet rays, and humidity, as represented in Fig. 5. Plastic pipes, sealant, and reinforced aluminum pellicle were used for such protection. This made it possible to significantly reduce the systematic inaccuracy of the coordinates that occur during the deformation of the points due to their uneven daily heating.

Only GNSS measurement data were used for the studies obtained from the beginning of the installation of the automated control system on February 9, 2016, to July 12, 2020, and were recorded each 30 s. The initial data turned out to be unreliable, as the system was being debugged during this period of operation. Therefore, measurements from July 2016 are used for calculations.

The GNSS time series analysis

As a result of the analysis of the time series of change of coordinates of the points defined by the GNSS method, it is established that in the data of the measurements processed by the GeoMoS software package, there are gross errors. This is especially evident at the beginning of the system, when it was set up, and when replacing equipment. Accordingly, these data required filtering. According to the time series, it is established that the average maximum value of the displacement in the horizontal plane and height relative to the middle position of the point for the whole period does not exceed 20 mm. Respectively, according to rule 3™, all values of deviations from the mean position of the point, which exceeded the absolute value of 60 mm, were filtered. The second step of filtering was to determine the average maximum displacement for the entire period separately for each point. Re-filtering eliminated displacements that were more than three times the mean maximum displacement in absolute terms.

Based on the filtered data, almost daily displacements of all GNSS points during the entire observation period were determined.

For example, Fig.6 shows the vertical displacement of the MP-11 point for the whole measurement period.

For other points, their displacement curves in the horizontal and vertical planes are similar. Although the amplitude of oscillations at each point is different, the displacement curves have a typical pattern. It consists in the fact that the displacements during each year have a smooth harmonic character, and extreme deviations relative to the dam axis are recorded annually in February (corresponding to 0.1 years from the beginning of the year) and in August (corresponding to 0.6 years from the beginning of the year).

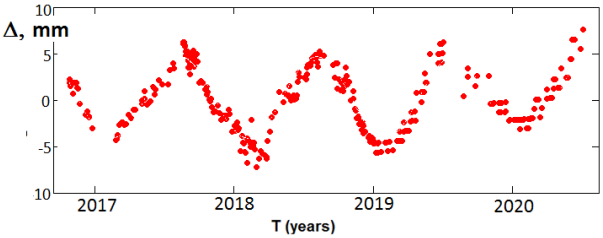

Fig. 6. Example of MP-11 displacements for the entire measurement period.

Consequently, displacements occur almost linearly during the six-month periods (from February to August). Therefore, it is necessary to consider the linear displacement rates of checkpoints within six months. Accordingly, the dataset was divided into half-yearly periods, and velocity vectors for half-yearly periods were given in the following calculations. A graphical representation of the velocity of horizontal displacements of points for half-year periods from 2016 to 2020 vectors distribution is given in Fig. 7.

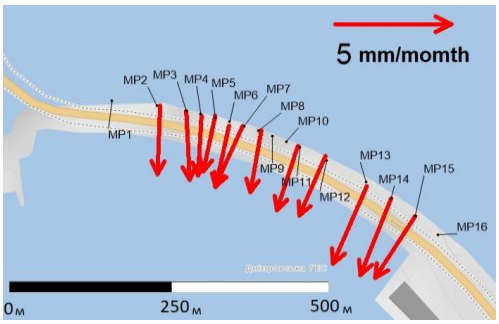

a – The period from June 2016 to January 2017

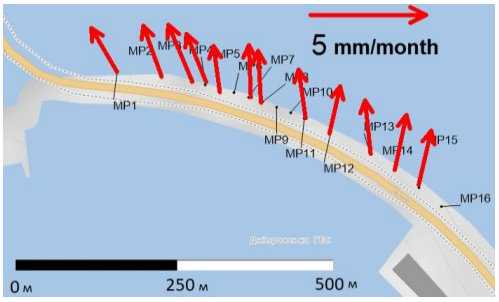

b – The period from January 2017 to June 2017

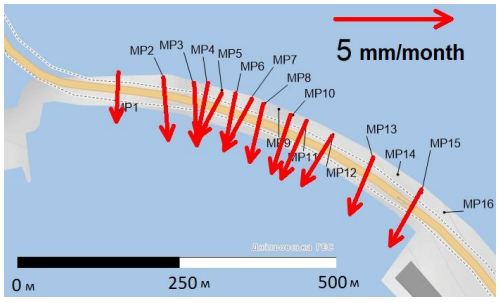

c – The period from June 2017 to January 2018

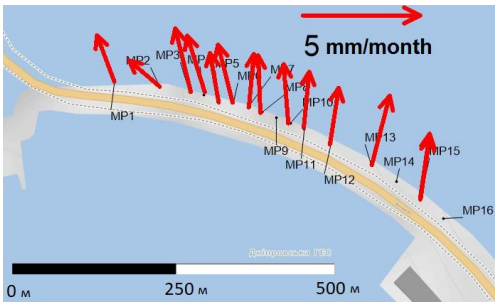

d – The period from January 2018 to June 2018

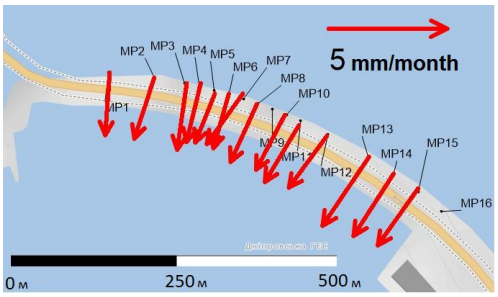

e – The period from June 2018 to January 2019

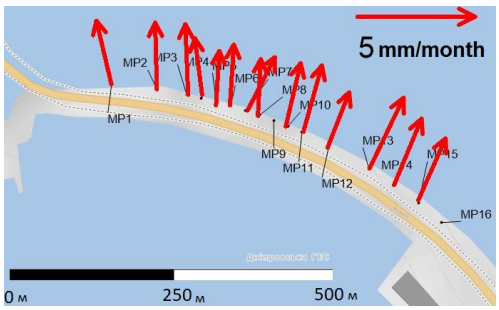

f – The period from January 2019 to June 2019

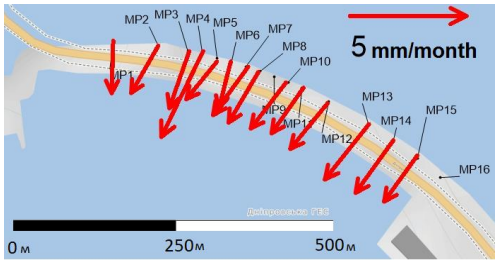

g – The period from June 2019 to January 2020

Fig. 7. Distribution of velocity of horizontal displacement vectors of control points of the Dnipro HPP dam from 2016 to 2020.

The velocity vectors of horizontal displacements (Fig. 7) during the annual period have a cyclical change of direction: in the first half of the year, the directions of velocity vectors of horizontal displacements are directed against the river, i.e., in the upper reaches, and the second – downstream. The amplitude of semi-annual horizontal oscillations of control points relative to the mean position ranges from 15–18 mm. Perpendicular location of the velocity vector of horizontal displacements to the axis of the arcuate dam prevails in all figures. Accordingly, in the first half of the year, the vectors of horizontal displacements aim to expand the dam, and in the second half of the year – at compression.

The velocities of vertical displacements for certain six-month periods are shown in Fig. 8.

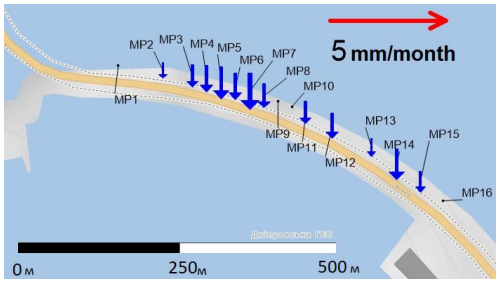

a – The period from June 2016 to January 2017

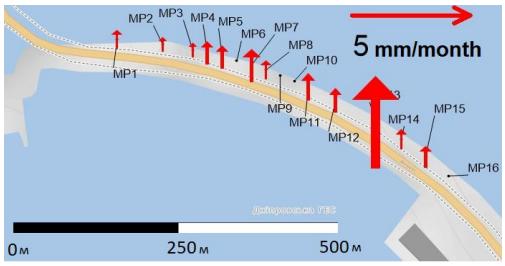

b – The period from January 2017 to June 2017

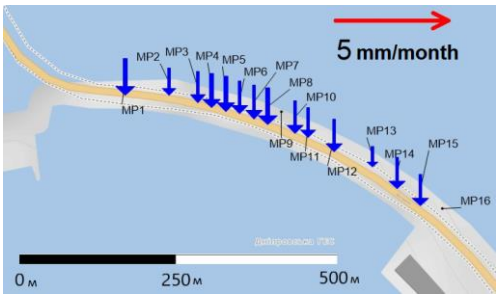

c – The period from June 2017 to January 2018

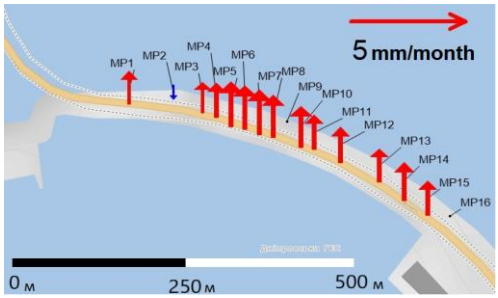

d – The period from January 2018 to June 2018

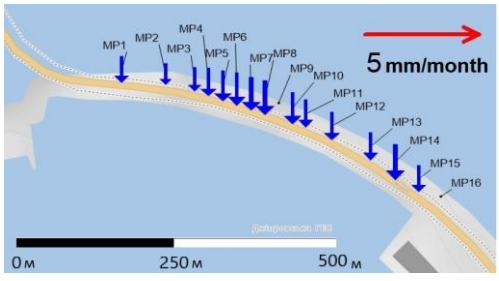

e – The period from June 2018 to January 2019

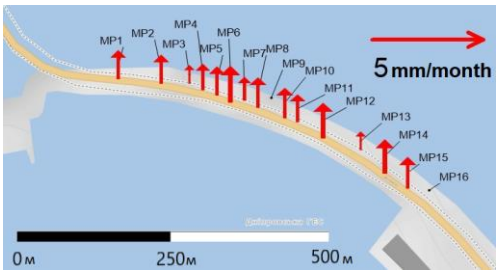

f – The period from January 2019 to June 2019

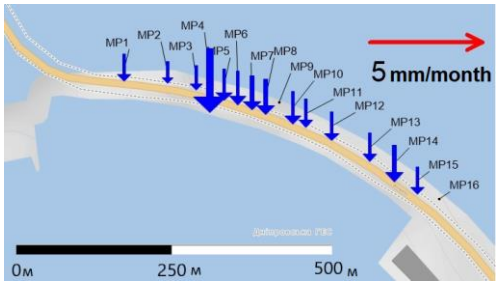

g – The period from June 2019 to January 2020

Fig. 8. Distribution of velocity of displacement vectors of control points of the Dnipro HPP dam from 2016 to 2020.

The velocities of vertical displacements for specific semi-annual periods are shown in Fig 8. The amplitude of semi-annual vertical oscillations of control points does not exceed 12–15 mm. Within these six-month periods, the shifts occur almost according to a linear law.

To determine the average amplitudes and periods of displacements of all control points throughout the observation time, their displacements were approximated by the following expression:

$$\Delta T_i = a_0 + a_1 \cdot \cos\left(\frac{T_i}{T}\right) + a_2 \cdot \sin\left(\frac{T_i}{T}\right), \qquad (1)$$

where $\Delta(T)_i$ – displacement; a_0, a_1, a_2 – approximation coefficients; T_i – running day from the beginning of the year; T – number of days per year.

Determination of the duration of the optimal period between the extreme displacements of the point was performed under the condition of the minimum standard error of the approximation

$$m = \sqrt{\frac{\sum \Delta^2}{n-1}} = \min, \qquad (2)$$

where Δ – deviation of the approximate offset relative to the measured.

Fig. 9 shows an example of finding the optimal period of displacement corresponding to the minimum of function (2) for item MP-4.

For each GNSS point, the approximation curves of vertical and horizontal displacements for the entire observation period are determined. For example (Fig. 10) shows the curve of approximation of displacements Δ according to the data of the whole observation period for the control point MP-11.

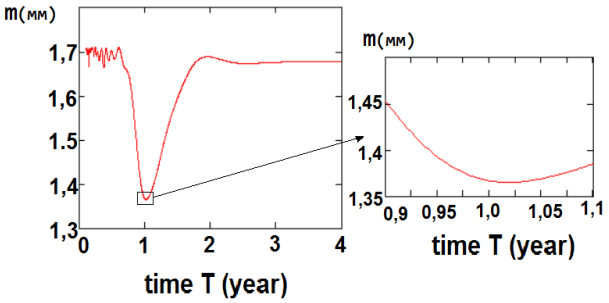

Fig. 9. The results of the search for the optimal period of displacements for item MP-4

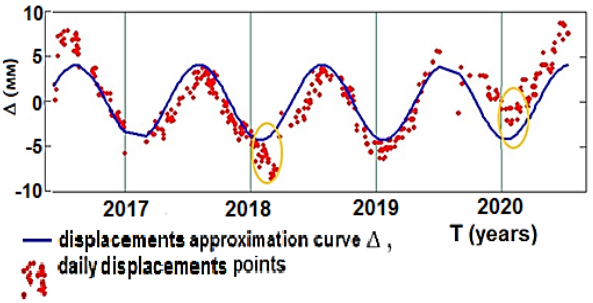

Fig. 10. The curve of displacement approximation ⊗ according to the data of the whole observation period for the control point MP-11.

The duration of the period of oscillations (Fig. 10) is close to one year. However, the difference between the optimal and annual periods leads to a systematic shift of the extremes of the approximated curve from the measured ones. These differences are indicated in Fig. 10 in yellow. The period of extreme changes of each point each year is different. Therefore, the length of the annual periods for each checkpoint was further investigated.

The results of determining the annual optimal periods of horizontal and vertical displacements for all points are given in the Tables 1, 2.

Table 1

Periods of horizontal displacements

Point name	Periods of horizontal displacements		
	2017	**2018**	**2019**
MP-1	1.064	0.956	1.058
MP-2	1.046	0.916	1.027
MP-3	1.033	0.963	1.011
MP-4	1.037	0.926	0.998
MP-5	1.078	0.935	1.016
MP-6	1.083	0.935	1.032
MP-7	1.124	0.943	1.012
MP-8	1.039	0.938	0.996
MP-10	1.058	0.,921	1.032
MP-11	1.026	0.941	0.995
MP-12	1.027	0.926	1.032
MP-13	1.091	0.954	1.05
MP-14	0.984	0.895	1.018
MP-15	0.863	0.947	1.021
Average	**1.040**	**0.935**	**1.021**

According to the average annual optimal periods of displacements of all points (Tables 1 and 2), the duration of the calculated optimal periods for all control points each year is different and not equal to one year. The time of the average annual periods of fluctuations of the displacements of control points during 2017–2019 varies in terms of days: for horizontal displacements – from 380 days to 341 days, and for vertical – from 400 days to 355 days.

Table 2

Periods of vertical displacements

Point name	Periods of horizontal displacements		
	2017	**2018**	**2019**
MP-1	1.204	0.970	0.972
MP-2	1.206	0.973	0.922
MP-3	1.198	0.975	0.987
MP-4	1.205	0.963	0.935
MP-5	1.040	0.991	0.988
MP-6	0.958	0.988	0.973
MP-7	0.992	0.992	0.946
MP-8	0.947	0.975	1.030
MP-10	0.965	0.956	1.043
MP-11	1.053	1.009	0.942
MP-12	1.179	0.997	0.973
MP-13	1.140	0.975	1.015
MP-14	1.239	0.896	1.021
MP-15	0.998	0.971	0.987
Average	**1.095**	**0.974**	**0.981**

Table 3

Epochs and magnitudes of extreme horizontal displacements of checkpoints in 2017

Point name	Winter		Summer	
	Day of the year	Displ. in mm	Day of the year	Displ. in mm
MP-1	54	-2.9	233	1.8
MP-2	55	-2.0	199	3.6
MP-3	54	-3.5	240	4.2
MP-4	59	-3.8	247	3.4
MP-5	54	-3.6	247	2.6
MP-6	54	-4.3	241	3.5
MP-7	49	-5.2	202	4.3
MP-8	54	-5.9	235	5.0
MP-10	55	-4.1	243	4.0
MP-11	54	-3.8	238	4.1
MP-12	60	-3.9	239	3.9
MP-13	54	-4.4	237	4.8
MP-14	54	-4.7	221	5.5
MP-15	76	-4.2	234	4.1
Average	**56**	**-4.0**	**233**	**3.9**

According to the calculations in tables 3–5, the epochs (days from the beginning of the year) are presented. Extreme horizontal displacements relative to the dam axis were observed at each point. Extreme deviations from the dam axis are positive in summer and negative in winter.

Histograms of extreme horizontal displacements for 2017–2019 are based on the data obtained in Fig. 11.

At almost all points (see Fig. 11), the maximum amplitude of oscillations is proportional to the magnitude of the annual displacements. Still, this pattern is preserved only in a separate comparison of summer and winter displacements. Almost all control points with large amplitude of displacement oscillations and an immense amount of displacement in the summer have small amplitude of oscillations and a small amount of displacement in the winter. A similar pattern is observed at points with small amplitude of displacement oscillations and a small amount of displacement in the summer. And in winter, at these points, there is large amplitude of displacement oscillations and a large amount of displacement.

Table 4

Epochs and magnitudes of extreme horizontal displacements of checkpoints in 2018

Point name	Winter		Summer	
	Day of the year	Displ. in mm	Day of the year	Displ. in mm
MP-1	95	-4.2	259	3.4
MP-2	59	-1.8	224	4.1
MP-3	53	-3.7	222	6.6
MP-4	64	-3.1	221	5.3
MP-5	66	-2.5	234	4.5
MP-6	62	-3.1	234	4.7
MP-7	62	-3.1	234	5.5
MP-8	58	-4.1	228	5.9
MP-10	66	-3.6	234	5.7
MP-11	53	-3.7	225	5.9
MP-12	56	-3.4	228	5.5
MP-13	44	-5.1	218	7.8
MP-14	51	-4.0	215	7.3
MP-15	49	-4.1	223	6.1
Average	**60**	**-3.5**	**229**	**5.6**

Table 5

Epochs and magnitudes of extreme horizontal displacements of checkpoints in 2019

Point name	Winter		Summer	
	Day of the year	Displ. in mm	Day of the year	Displ. in mm
MP-1	30	-2.2	235	7.6
MP-2	28	-2.8	235	5.8
MP-3	44	-2.8	235	8.4
MP-4	53	-2.0	235	6.0
MP-5	47	-1.9	237	5.6
MP-6	39	-2.4	237	6.1
MP-7	45	-2.2	246	6.2
MP-8	39	-1.5	238	4.5
MP-10	37	-2.5	226	7.0
MP-11	37	-2.6	237	6.8
MP-12	34	-1.9	237	6.4
MP-13	16	-2.6	235	8.4
MP-14	31	-2.6	245	7.8
MP-15	34	-2.3	246	6.6
Average	**37**	**-2.3**	**237**	**6.7**

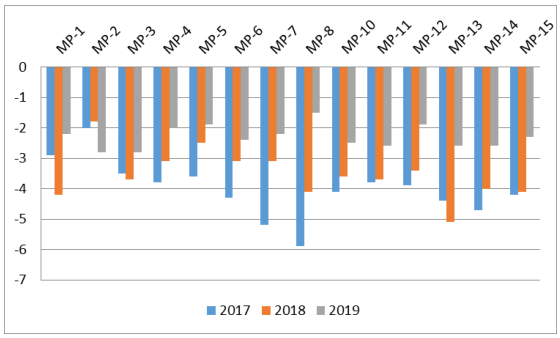

a – winter displacements

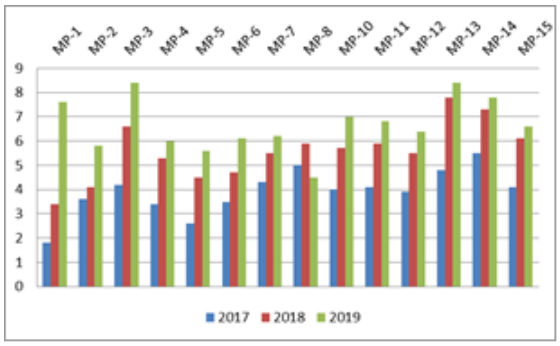

b – summer displacements

Fig. 11. The value of extreme horizontal displacements of checkpoints for 2017–2019.

At almost all points (see Fig. 11), the maximum amplitude of oscillations is proportional to the magnitude of the annual displacements. Still, this pattern is preserved only in a separate comparison of summer and winter displacements. Almost all

Fig. 12 shows the values of seasonal (winter and summer) average horizontal displacements of checkpoints for 2017-2019.

Fig. 12 shows the representation of the annual patterns of distribution of average seasonal displacements along the axis of the dam. In winter and summer, the horizontal displacements increase in waves from the right edge of the dam to its left edge. This is confirmed by the symmetry of the lines of the conditional distribution of displacements along the axis of the dam (Figs. 12a and 12b). The revealed regularities may be a consequence of the compression of the dam body and the appearance of stresses during the horizontal winter shift, caused by the partial concentric direction of the displacement vectors inside the lower reservoir. According to the magnitude of the accumulated tensions in the dam's body in the winter, their corresponding unloading occurs in a partially radial direction of the vectors relative to the axis of the dam towards the upper reservoir in the summer. The greater the accumulation of stresses in the dam's body in the winter, the greater the length of the vectors of horizontal displacements in the summer. This is necessary to relieve the stresses. In addition, of course, the magnitude of winter and summer shifts is also affected by rising ambient temperatures. A similar but reverse process is represented in the transition of deformations from summer to winter.

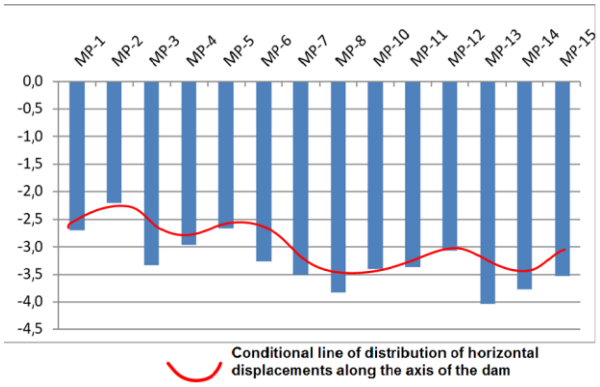

a – winter displacemens

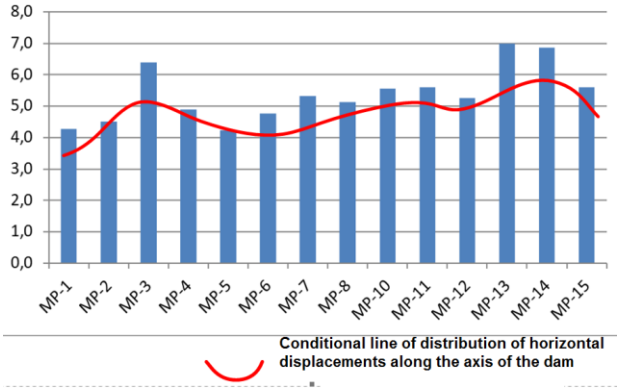

b – summer displacements

Fig. 12. The value of the average horizontal displacements of control points for 2017–2019.

Similar calculations were performed for vertical displacements, according to the results of analyses in the table. Fig.s 7 to 9 show the epochs (days from the beginning of the year) in which extreme vertical displacements relative to the dam axis were observed at each point. Extreme deviations from the dam axis are positive in summer and negative in winter.

Based on the obtained data, Fig. 13 presents histograms of extreme vertical displacements for 2017–2019.

Table 7

Epochs and magnitudes of extreme vertical displacements of checkpoints in 2017

Point name	Winter		Summer	
	Day of the year	Displ. in mm	Day of the year	Displ. in mm
1	2	3	4	5
MP-1	-4*	-1.2	216	1.2
MP-2	-28	-0.5	196	1.03
MP-3	-6	-1.2	218	1.9
MP-4	-6	-1.9	214	1.2
MP-5	54	-1.9	232	1.5

Continuation of Table 7

1	2	3	4	5
MP-6	54	-3.2	238	2.0
MP-7	59	-3.5	240	2.2
MP-8	54	-1.7	227	1.6
MP-10	55	-1.7	218	1.8
MP-11	54	-1.4	231	1.7
MP-12	-4	-1.6	223	2.0
MP-13	61	-1.5	234	1.9
MP-14	-4	-1.7	231	1.7
MP-15	95	-1.5	242	1.5
Average	**31**	**-1.7**	**226**	**1.7**

* A negative value in the collocation of days of the year indicates that the maximum deviation occurred before the beginning of the year on the specified number of days (for example, for item MP-1 in 2017, day -4 corresponds to the epoch of 28.12.2016).

Table 8

Epochs and magnitudes of extreme vertical displacements of checkpoints in 2018

Point name	Winter		Summer	
	Day of the year	Displ. in mm	Day of the year	Displ. in mm
MP-1	53	-1.2	222	2.1
MP-2	51	-1.5	221	2.4
MP-3	41	-1.8	223	3.5
MP-4	48	-2.2	234	3.3
MP-5	51	-2.1	234	3.7
MP-6	41	-2.1	220	3.1
MP-7	53	-2.0	228	3.2
MP-8	48	-1.7	228	2.5
MP-10	41	-1.5	220	2.7
MP-11	53	-1.5	233	1.2
MP-12	61	-1.8	225	3.2
MP-13	35	-1.6	215	2.2
MP-14	53	-1.2	222	2.1
MP-15	51	-1.5	221	2.4
Average	**49**	**-1.7**	**225**	**2.7**

Table 9

Epochs and magnitudes of extreme vertical displacements of checkpoints in 2019

Point name	Winter		Summer	
	Day of the year	Displ. in mm	Day of the year	Displ. in mm
MP-1	43	-0.8	235	2.1
MP-2	66	-1.1	234	1.5
MP-3	73	-0.9	246	1.6
MP-4	63	-0.8	235	1.8
MP-5	39	-0.9	237	1.8
MP-6	61	-1.3	237	3.4
MP-7	77	-0.9	246	2.1
MP-8	35	-1.0	238	2.1
MP-10	47	-0.8	237	2.1
MP-11	62	-0.8	237	2.1
MP-12	54	-1.0	237	3.3
MP-13	51	-0.8	246	1.5
MP-14	41	-1.4	245	2.8
MP-15	34	-0.8	246	2.0
Average	**53**	**-1.0**	**240**	**2.2**

At almost all points (see Fig. 13), the maximum amplitude of oscillations is proportional to the magnitude of the annual displacements. But this pattern, similar to horizontal displacements, is preserved only by an independent comparison of summer and winter vertical displacements.

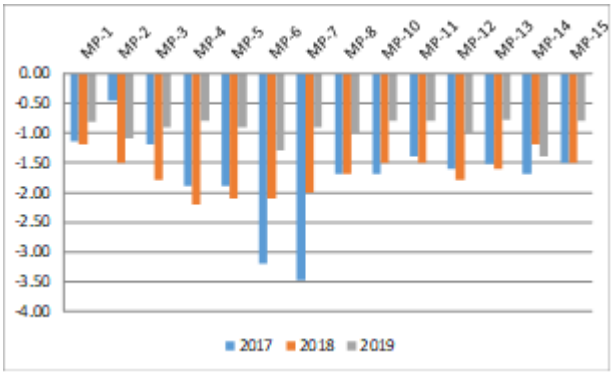

a – Extreme winter displacements

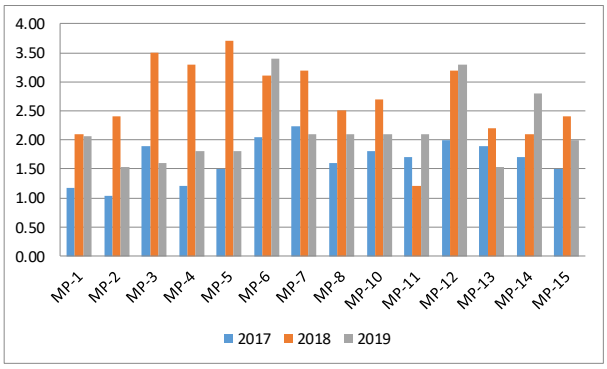

b – Extreme summer displacements

Fig. 13. The value of the maximum vertical displacements.

Fig. 14 shows the values of seasonal (winter and summer) average horizontal displacements of checkpoints for 2017–2019. The representation of the annual patterns of distribution of average seasonal displacements along the axis of the dam is obvious. In winter and summer, the vertical displacements increase from the edges of the dam to its central part. Similar patterns were obtained on other HPPs, particularly on the dam of HPP Lijiaxia in China [Zhang. et al., 2018]. In addition, similar to horizontal displacements, there is asymmetry of the lines of the conditional distribution of displacements along the axis of the dam (Figs. 14a and 14b.). The only partial exception is paragraph MP-12.

The identified patterns may be the result of vertical compression of the dam body and the appearance of maximum stresses in its central part, caused by an increase in the vertical displacement in the direction of the middle of the dam. According to the magnitude of the accumulated stresses in the dam's body in the winter, there is the corresponding unloading by the partial expansion of the dam's body in the vertical direction in the summer. Like horizontal stresses, the greater the accumulation of vertical stresses in the dam body in winter, the greater the length of the perpendicular

displacement vectors in summer, which is necessary to relieve these stresses. In addition, the increase in ambient temperature also undoubtedly affects the magnitude of the displacements. Probably in the central part of the dam, these temperature differences are much more significant, so in the middle of the dam recorded larger amplitudes of winter and summer shifts.

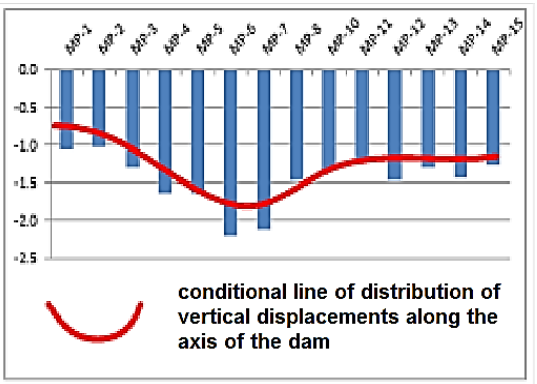

a – winter displacements

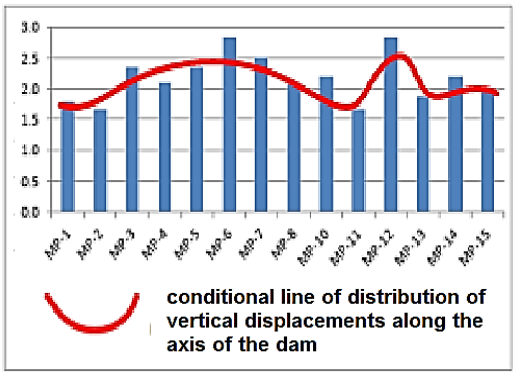

b – summer displacements

Fig. 14. The value of the average vertical displacements of control points for 2017–2019.

Undoubtedly, one of the leading causes of such cyclic deformations of the dam is the seasonal change in ambient temperature [Oro, SR., Et al., 2016, Zhang, et al., 2018; Mata J. et al., 2013, et al.].

To establish the spatio-temporal relationship between the displacement vectors of the dam control points with air temperature, we analyzed the changes in the annual air temperature near the dam during 2017–2019.

For the generalization of seasonal temperature changes, we have approximated the same function (1) the time series of temperature values obtained from the meteorological station located directly at the Dnipro HPP. These temperatures come with the discreteness of 3 hours, starting from 2 hours to 23 hours each day.

According to the approximation, it is established that the average period of extreme temperature fluctuations according to 2017–2019 is almost one year (0.999).

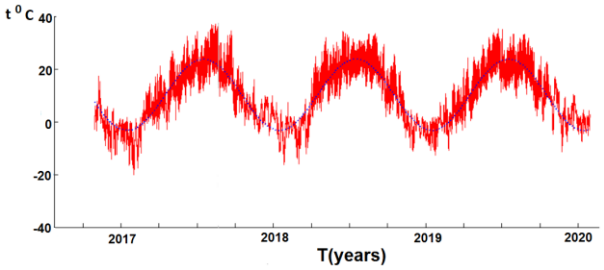

Fig. 15. Temperatures change from 2017 to 2019 (according to the meteorological station of the Dnipro HPP).

However, a detailed analysis of individual annual temperature changes shows that the length of the period between the approximated temperatures is different each year.

Table 10 shows the epochs from the beginning of the year of fixing the extreme values of horizontal and vertical displacements and temperature extremes.

Table 10

Epochs of extreme horizontal and vertical displacements of control points and air temperatures

Year	Epochs (days from the beginning of the year)					
	Horizontal displ.		Vertical displ.		Temperature	
	Win	Smr	Win	Smr	Winter	Smr
2017	56	233	31	226	13	197
2018	60	229	49	225	22	193
2019	37	237	53	240	6	200

Table 11 shows the approximate values by expression (1) extreme air temperatures from 2017 to 2019.

Table 11

Values of approximate extreme air temperatures from 2017 to 2019

Year	Min	Max
2017	-4.04	23.50
2018	-3.88	24.32
2019	-1.82	23.40

The differences between epochs, extreme displacements of control points, and epochs of extreme air temperatures were calculated based on the obtained data. The differences between them are given in Table 12.

Table 12

Differences of epochs of extreme displacements of control points and extreme air temperatures

Year	Epoch differences (days)			
	For horizontal displ.		For vertical displ.	
	Win	Smr	Win	Smr
2017	43	36	18	29
2018	38	36	27	32
2019	31	37	47	40
Average	37.3	36.3	30.7	33.6

Epochs of extreme horizontal displacements (Table 12) occur later than epochs of extreme air temperatures by an average of 37 days. In this case, the higher the extreme temperature in winter, the smaller the difference between the epochs. In the summer, the extreme temperature for three years was almost unchanged, and, accordingly, the difference between the epochs was also almost constant. For vertical displacements, this difference in epochs, on the contrary, increases in winter with an increase in extreme temperature. For summer periods, the difference in epochs also increases at almost constant extreme temperatures. On average, epochs of extreme vertical displacements occur compared to epochs of extreme air temperatures with a delay of 32 days. The temperature deformations of the dam are related to the temperature of concrete structures, which has to change with an inevitable delay relative to the air temperature.

The conducted research allows for establishing the periods and sizes of seasonal deformations of the dam of the Dnipro hydroelectric power station and the influence of air temperatures on them. These deformations have a significant impact on the appearance of cracks in the dam's body and its stability. The magnitude of extreme displacements and the epoch of their manifestation depend on the dam's design and its technical parameters. For each dam, these excessive displacements and the periods of their representation will be different. Accordingly, monitoring these displacements and their changes over time is one of the criteria for assessing the general condition of the dam.

The regularities of the connection between temperature change and GNSS displacements of the points revealed from the conducted research can be used for further investigations on processing and analysis of monitoring data of engineering constructions.

Conclusions

Based on the research, the following conclusions can be drawn.

1. The influence of ambient temperature has a decisive effect on the cyclicity of dam deformations. This applies to both horizontal and vertical displacements but in the absence of significant changes in the water level in the upper reservoir.

2. According to the data of the three-year GNSS monitoring of the Dnipro HPP dam, the amplitude of semi-annual horizontal oscillations of the control points relative to the dam axis is in the range of 15–18 mm. Almost all vectors of horizontal displacements are perpendicular to the axis of the arcuate dam. In the first half of the year, the vectors of horizontal displacements aim to expand the dam, and in the second half of the year – at compression. In winter and summer, the horizontal displacements increase in waves from the right edge of the dam to its left edge.

3. For vertical displacements, it was established that every year in the first half of the year, all dams are raised, and in the second half – all points are lowered. The amplitude of semi-annual vertical oscillations of control points is in the range of 12–15 mm. In winter and summer, the vertical displacements increase from the edges of the dam to its central part.

4. The detected patterns may result from vertical compression of the dam body and the appearance of maximum stresses in its central part, caused by an increase in the vertical shear in the direction of the middle of the dam. According to the magnitude of the accumulated stresses in the dam's body in the winter, there is the corresponding unloading by the partial expansion of the dam's body in the vertical direction in the summer. In addition, the increase in ambient temperature also undoubtedly affects the magnitude of the displacements. In the central part of the dam, these temperature differences are much more significant. So larger amplitudes of winter and summer vertical displacements are recorded in the middle of the dam.

5. Epochs of extreme horizontal displacements occur later than epochs of extreme air temperatures by an average of 37 days. On average, the periods of excessive vertical displacements arise compared to the epochs of extreme air temperatures with a delay of 32 days. The temperature deformations of the dam are related to the temperature of concrete structures, which changes with a certain delay relative to the air temperature.

6. The magnitude of extreme displacements and the epoch of their manifestation depend on the dam's design and its technical parameters. For each dam, these excessive displacements and the epochs of their representation will be different. Accordingly, monitoring these displacements and their changes over time is one of the criteria for assessing the general condition of the dam.

References

Chen, Y. Q., Chrzanowski, A., & Secord, J. M. (1990). A strategy for the analysis of the stability of reference points in deformation surveys. *CISM Journal*, *44*(2), 141–149.

Chrzanowski, A., Szostak, A., & Steeves, R. (2011, October). Reliability and efficiency of dam deformation monitoring schemes. *In Proceedings of the CDA 2011 Annual Conference. Fredericton, NB.* Canada. October (pp. 15–20).

Corsetti, M., Fossati, F., Manunta, M., & Marsella, M. (2018). Advanced SBAS-DInSAR technique for controlling large civil infrastructures: An application to the Genzano di Lucania dam. *Sensors*, *18*(7), 2371.

Drummond, P. (2010, April). Combining Cors Networks, Automated Observations and Processing, for Network Rtk Integrity Analysis and Deformation Monitoring. In *Proceedings of the 15th FIG Congress Facing the Challenges, Sydney, Australia* (p. 11–16).

Khosravi, S., & Heydari, M. M. (2013). Modelling of concrete gravity dam including dam-water-foundation rock interaction. *World Appl. Sci. J*, *22*, 538–546.

Mata, J., de Castro, A. T., & da Costa, J. S. (2013). Time–frequency analysis for concrete dam safety control: Correlation between the daily variation of structural response and air temperature. *Engineering structures*, *48*, 658–665.

Milillo, P., Bürgmann, R., Lundgren, P., Salzer, J., Perissin, D., Fielding, E., ... & Milillo, G. (2016). Space geodetic monitoring of engineered structures: The ongoing destabilization of the Mosul dam, Iraq. *Scientific reports*, *6*(1), 1–7.

Moroko, V. M. (2010). Dniproges: Black August 1941. Scientific works of the historical faculty of Zaporizhia National University. Iss. XXIX. P. 197–202.

National report on the state of man-made and natural security in 2013 Access mode: http:/ www.mns.gov.ua/content/annual_report_ 2013.html.

Oro SR, Mafioleti TR, Neto AC, Garcia SRP, Júnior CN Investigation of the influence of temperature and water level of a reservoir on the displacement of a concrete dam. *International J. Appl. Fur. Eng. 2016; 21: 107–120.* https://cyberleninka.org/article/n/1341354.pdf.

Sarkar, R., Paul, D. K., & Stempniewski, L. (2007). Influence of reservoir and foundation on the nonlinear dynamic response of concrete gravity dams. *ISET Journal of Earthquake technology*, *44*(2), 377–389.

Scaioni, M., Marsella, M., Crosetto, M., Tornatore, V., & Wang, J. (2018). Geodetic and remote-sensing sensors for dam deformation monitoring. *Sensors*, *18*(11), 3682.

Tretyak, K., Periy, S., Sidorov, I., & Babiy, L. (2015). Complex High Accuracy Satellite and Field Measurements of Horizontal and Vertical Displacements of Control Geodetic Network on Dniester Hydroelectric Pumped Power Station (HPPS). *Geomatics and environmental engineering*, *9*(1). 83–96. http://dx.doi. org/10.7494/geom.2015.9.1.83.

Ukrhydroenergo News. Safety of dams. https://uhe.gov.ua/en/node/5207.

Zeidan, B. A. (2015, March). Effect of foundation flexibility on dam-reservoir-foundation interaction. *In Proceedings of the Eighteenth International Water Technology Conference*, Sharm El Sheikh, Egypt (p. 12–14). https://www.researchgate.net/publication/280308540.

Zhang, L., Peng, M., Chang, D., & Xu, Y. (2016) *Dam Failure Mechanisms and Risk Assessment*; John Wiley & Sons: Hoboken, NJ, USA, 2015; ISBN 9781118558522.

Zhang, Y., Yang, S., Liu, J., Qiu, D., Luo, X., & Fang, J. (2018). Evaluation and Analysis of Dam Operating Status Using One Clock-Synchronized Dual-Antenna Receiver. *Journal of Sensors, 2018*.

Корнилій ТРЕТЯК[1], Богдан ПАЛЯНИЦЯ[1]

[1*] Кафедра вищої геодезії та астрономії, Національний університет “Львівська політехніка”, вул. С. Бандери, 12, Львів, 79013, Україна, ел. пошта: bohdan.b.palianytsia@lpnu.ua

ДОСЛІДЖЕННЯ СЕЗОННИХ ДЕФОРМАЦІЙ ГРЕБЛІ ДНІПРОВСЬКОЇ ГЕС ЗА ДАНИМИ ГНСС ВИМІРІВ

Мета. Виявити залежність між сезонною зміною температури і вертикальними та горизонтальними зміщеннями контрольних ГНСС пунктів на основі даних, отриманих автоматизованою системою моніторингу греблі Дніпровської ГЕС у період з 2016 по 2020 роки. Вихідні дані. Для досліджень використовувалися дані цілодобових ГНСС вимірів, отриманих на 16 пунктах греблі Дніпровської ГЕС у період з середини 2016 до середини 2020 року. Методика. Часові ряди ГНСС вимірів, попередньо опрацьованих системою GeoMoS, проаналізовані спеціально розробленим програмним продуктом на предмет визначення параметрів сезонних зміщень та їх взаємозв’язку із сезонними змінами температури повітря. Результати. На основі досліджень встановлено, що на циклічність деформацій дамби визначальним є вплив температури довкілля. Це стосується як горизонтальних, так і вертикальних зміщень, але при умові відсутності суттєвих змін рівня води у верхньому водосховищі. Значення екстремальних зміщень зростають ближче до середини греблі і спадають на краях. Така тенденція простежується щорічно. За даними трирічного ГНСС моніторингу греблі амплітуда піврічних горизонтальних коливань контрольних пунктів відносно осі греблі є в межах 15–18 мм. Практично усі вектори горизонтальних зміщень мають перпендикулярне розташування до осі дугоподібної греблі. У першій половині року вектори горизонтальних зміщень спрямовані на розширення греблі, а у другій половині року – на стиснення греблі. У зимовий та літній період горизонтальні зміщення хвилеподібно зростають від правого краю греблі до її лівого краю. Встановлено, що практично кожного року екстремальні відхилення, як горизонтальні так і вертикальні, відбуваються у лютому та серпні місяці. Екстремуми температури наступають швидше, ніж екстремальні зміщення ГНСС станцій. Для греблі Дніпровської ГЕС горизонтальні екстремальні зміщення в середньому відстають на 37 діб, а вертикальні – на 32 доби від екстремальних температур. Очевидно температурні деформації греблі пов’язані з температурою бетонних конструкцій, яка змінюється з певним запізненням відносно температури повітря. Величини екстремальних зміщень і епохи їх прояву залежать від конструкції греблі і її технічних параметрів. Для кожної греблі ці екстремальні зміщення і епохи їх прояву будуть різними. Відповідно моніторинг цих зміщень і їхніх змін у часі є одним із критеріїв оцінки загального стану греблі. Наукова новизна та практична значущість. Виявлені у результаті проведених досліджень закономірності зв’язку між зміною температури та зміщеннями ГНСС пунктів можуть бути використані для подальших досліджень з опрацювання та аналізу даних моніторингу гідротехнічних споруд.

Ключові слова: ГНСС виміри, геодезичний моніторинг гідротехнічних споруд, геодезичний моніторинг Дніпровської ГЕС.

Received 15.03.2021